Title

Use of self-organizing maps for exploring coordination variability in the transition between walking and running

Permalink

https://escholarship.org/uc/item/4s43n24d

Journal

International Journal of Comparative Psychology, 27(2)

ISSN

0889-3675

Authors

Bartlett, Roger M
Lamb, Peter F
O'Donovan, David
et al.

Publication Date

2014

DOI

10.46867/ijcp.2014.27.02.06

Copyright Information

Peer reviewed

Use of Self-Organizing Maps for Exploring Coordination Variability in the Transition Between Walking and Running

Roger Bartlett
University of Otago, New Zealand

Peter Lamb
University of Otago, New Zealand
Technische Universität München, Germany

David O'Donovan and Gavin Kennedy
University of Otago, New Zealand

This study investigated multi-dimensional coordination instability and variability in the transitions between walking and running for a 26 year old female runner using self-organizing maps (SOMs) in three experimental procedures. We found different multi-dimensional coordination patterns for walking and running using the output from SOMs as stride trajectories on U-matrices and attractor diagrams. In transient conditions, the participant showed multi-stability, or instability, in the transition region for decreasing but not for increasing speeds. She also clearly showed increased multi-dimensional coordination variability around the transition region only for decreasing speeds and only in transient conditions. These findings may not be general across runners nor were they conclusive enough to support variability as a facilitator of the change from running to walking. Self-organizing maps provide us with a tool to study multi-dimensional coordination (and coordination variability) and to reduce its complexity to relatively simple map outputs, including basins of attraction and attractor landscapes.

Models of the sudden change of gait coordination modes in human locomotion have been based on mechanical and energetic mechanisms, which attempt to increase energy efficiency or reduce mechanical stress on the system. However, as Diedrich and Warren (1995) have pointed out, the predictions of these models do not agree with experimental results. An attractive theoretical framework for addressing the qualitative changes in human coordination comes from pattern formation in complex systems. Central to this perspective is that emergent coordination patterns are a result of nonspecific, self-organizing dynamics of the system, as opposed to top-down motor programs. The spontaneous, qualitative switch in gait modes is triggered by one stable mode, or attractor, becoming unstable, thus requiring the system to reorganize and find a new attractor. These transitions not only serve to reduce energy requirements when changing locomotion speeds, but also afford the system flexibility in unique or changing environments. The instabilities which spark the switches in gait are empirically observed as a sudden increase in movement variability. Some authors (e.g., Diedrich & Warren, 1995; 1998; Segers, Aerts, Lenoir, & De Clercq, 2006) have noted an increase in movement or coordination variability as the transition from one form of gait to another is approached, which is consistent with the findings for bi-manual coordination of Kelso and his co-workers (see Kelso, 1995). Similar to bi-manual coordination, with gait, the changing locomotion speed can be thought of as a control parameter which can force the movement system through various states of stability, represented by a single collective variable. Relative phase (see Hamill, Haddad, & McDermott, 2000) between two joint angles (or two segment angles) has most frequently been used in the literature to characterize coordination in

terms of a collective variable (e.g., Diedrich & Warren, 1995; Li, van den Bogert, Caldwell, van Emmerik, & Hamill, 1999; Seay, Haddad, van Emmerik, & Hamill, 2006).

By contrast, other researchers have not found this increase in variability leading up to the transitions between walking and running (e.g., Kao, Ringenbach, & Martin, 2003; Seay et al., 2006). It is worth noting here that coordination in walking and running is multi-dimensional, involving the joints of all four limbs as well as the pelvis, trunk and head in all three cardinal planes. Kao et al. (2003) suggested that the additional task constraint of postural control altered intra-limb coordination dynamics enough to explain the discrepancy between their results and those of the classical bi-manual coordination studies (e.g., Haken, Kelso, & Bunz, 1985). Others have suggested that inter-limb, rather than intra-limb coordination, show the expected loss of stability leading up to the transition speeds (Haddad, van Emmerik, Whittlesey, & Hamill, 2006; Seay et al., 2006). Such multi-dimensional coordination has rarely been studied, largely because of the few tools available (see also Lamoth, Daffertshofer, Huys, & Beek, 2009). In order to investigate whether coordination instability does indeed trigger the switch between gait modes, more comprehensive representations that may account for such task constraints as postural control should be embraced.

Self-organizing maps (SOMs, a type of artificial neural network) are a tool for reducing high-dimensional datasets, such as those produced when investigating human motion using three-dimensional motion-capture systems. The non-linear properties of SOMs reduce redundancies in datasets and enable high-dimensional data to be mapped onto low-dimensional output maps for interpretation (e.g., Bauer & Schöllhorn, 1997; Barton, Lees, Lisboa, & Attfield, 2006; Lamb, Bartlett, & Robins, 2010, 2011). Of particular use and importance is that topological relationships in the original dataset are preserved by the SOM procedure; for example, movement phases and the key events that separate them are easily identifiable on the SOM output maps.

We hypothesized that the SOM analysis would show increased multi-dimensional coordination variability towards the gait transition region, in confirmation of some, but not all, previous findings based on relative phase. We also hypothesized that the SOM would enable us to identify attractor diagrams (as in Lamb et al., 2011) and that there would be separate attractors for walking and running, with possible multi-stability in the transition region. Attractor diagrams for walking and running have not previously been produced from experimental data. As the transition from walking to running occurs frequently in sport, this research is very sport relevant.

Method

Participant

The participant in this extended case study was a 26 year old female who was a regular runner, running at least 3-4 times a week and competing in short and middle distance club events on weekends. Ethical clearance already existed at the University of Otago for this type of study, through a three-year course approval.

Procedure

The rigid-body model that we used consisted of 15 segments (head, thorax, humerus [left and right], forearm [left and right], hand [left and right], pelvis, thigh [left and right], shank [left and right], and foot [left and right]. Sixty-three retro-reflective markers (15 mm and 10 mm in diameter) were used to define segments and local joint coordinate systems (Figure 1). Joint centers were mostly located at the midpoint of a line joining lateral and medial markers. Glenohumeral and hip joint centers were estimated by calculation of the pivot point of the instantaneous helical axes method (Schwartz & Rozumalski, 2005). This calculation was performed in Visual3D (C-Motion Inc., Germantown, MD) on functional range of motion trials for each arm and leg (Begon, Monnet, & Lacouture, 2007). The right-handed orthogonal system defines the vertical or longitudinal axis as Z; the anteroposterior axis as Y; and the mediolateral axis as X; these axes represent axial rotations (Z); ab-adduction (Y); and flexion-extension (X) at most joints. All rotation orders were represented by Cardan sequences (e.g., X-Y-Z, Z-X-Y).
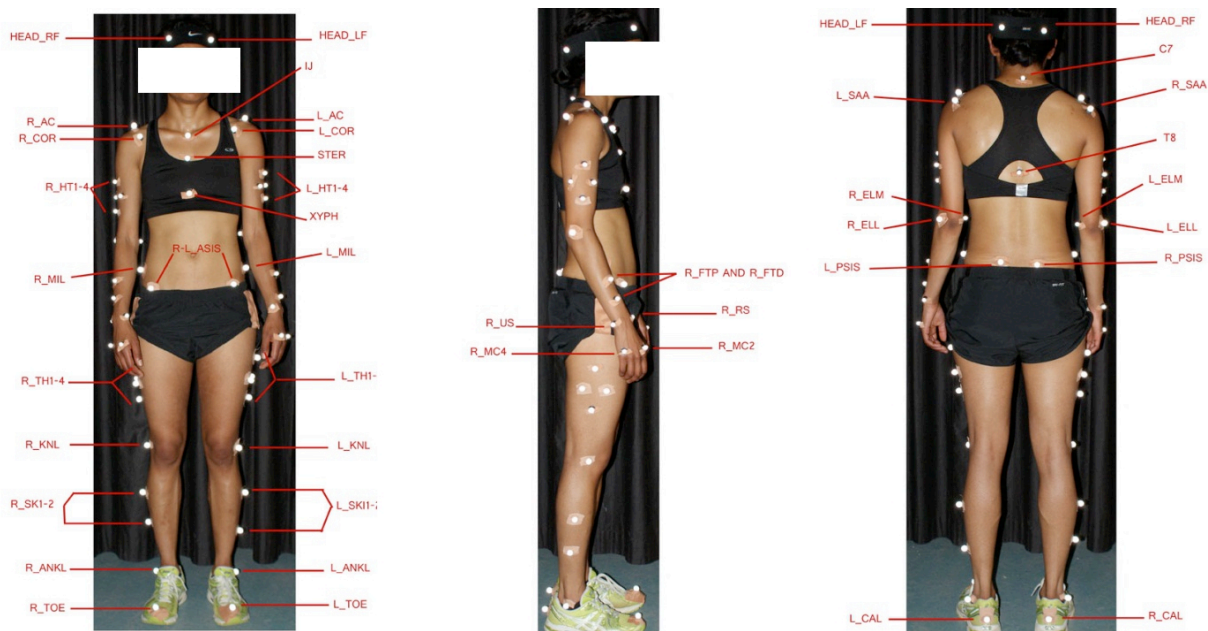
Figure 1. Marker set used: front, side and rear views.

A 10-camera three-dimensional motion analysis system (Vicon, Oxford, UK) sampling at 200 Hz captured the positions of markers. Assessment of camera residuals (reconstruction accuracy) took place after calibration; if any camera had residuals > 1.0 mm, the calibration was repeated until a satisfactory residual (< 1.0 mm) was achieved. Data were collected at the University of Otago, School of Physical Education Biomechanics Laboratory. On arrival the participant was briefed on experimental procedures and gave informed consent to participate.

The first (steady state) procedure began with a six minute warm-up, during which the participant identified her preferred walking and running speeds on a level treadmill. The speed at which the walk-to-run transition occurred was also identified. Based on this range of speeds, 18 speeds were selected from 2.5 to 16.0 km/h. The transition region was bordered by speeds of 7.5 km/h, and 8.0 km/h. The trial order was randomized to minimize any step-wise practice effects. For each trial the participant was given a one-minute familiarization before data capture began. Twenty to 25 strides at each speed were collected, with 10 strides being randomly selected for further analysis in post-processing. Between trials the participant was given one minute of recovery time to minimize the potential effect of fatigue.

In the second (transient) procedure, on a separate day, the participant walked or ran at speeds from 6.2 to 9.2 km/h in 0.2 km/h steps with the belt speed increasing and then decreasing. The smaller speed increments and narrower range compared to the first procedure allowed a more detailed investigation of the transition region. Accelerating from the slowest speed to the highest and vice versa allowed us to observe the change in coordination as a result of a gradual and relatively continuous change in speed. Data were collected for 30 s immediately after the belt had reached the new speed (see also Bartlett, O'Donovan, Kennedy, & Saini, 2012).

A third, mixed, procedure, also on a separate day, was a combination of the other two, including both transient and steady state, but without the randomization used in the first procedure. This procedure extended the previous case study of Bartlett et al. (2012), which showed unexpected changes in coordination in the transient procedure with decreasing belt speed. Based on the previous two procedures, belt speeds in the mixed procedure were chosen to focus even more on the gait transition region, particularly for decreasing speeds, so we used 4.3, 5.1, 6.0, 7.0, 7.4, 7.6 km/h, then 0.2 km/h increments increasing and 0.1 km/h decreasing to 8.6 km/h, then 9.0, 10.0, 12.6 and 14.5 km/h with as long a rest as the participant wanted between the increasing and decreasing speed conditions.

Local segment coordinate systems were established, and functional joint centers (Schwartz & Rozumalski, 2005) and joint angles were calculated before angle data were exported for further processing, such as key event identification, using custom MATLAB (Mathworks, Natick, MA) routines. Analysis of residuals informed the use of a fourth-order zero-lag Butterworth low-pass filter with a 10 Hz cut-off frequency. Key foot events (toe-off and touchdown) were identified in MATLAB by finding local minima in the vertical spatial position of foot markers at the calcaneus and on the shoe above the head of the second metatarsal. After event identification and

visual inspection, trials were trimmed to individual strides, beginning and ending at right toe-off. Angular velocities were calculated using differentiation of joint angle data. Individual strides were saved for later input into the SOM procedure. Strides were range-normalized to maximum and minimum values of +1 and -1 respectively for angle data, and +1 or -1 for angular velocity data, before being time normalized to 100 data points in both instances (Kohonen, 2001; Vesanto, Himberg, Alhoniemi, & Parkankangas, 2000). A SOM (see details below) was trained for each of the experimental procedures using all of the normalized data for all angles and angular velocities for each speed, for 10 random strides for the first procedure and for the first 20 strides for the second and for the first (transient) and last (steady state) 20 for the third.

Self-Organizing Maps

Self-organizing maps are a tool for clustering (usually high-dimensional) data and visualizing the clusters on a low-dimensional output map (see Kohonen, 1982; 2001). As mentioned above, the analyses of human movement are complicated by the high-dimensional time-series data that describe the movements. The variables are often, as is the case with this case-study, joint angles and their angular velocities. SOMs provide a method for visualizing the relationship among the original variables, throughout the movement, while maintaining the original topological relationships within the data. In the following subsection we will provide an overview of the SOM algorithm and methods for visualizing the output.

SOM architecture. The basic architecture of a SOM consists of a layer of output nodes fed forward by a layer of input nodes (Figure 2). Input nodes are represented by input vectors. A given input vector represents a time sample from the dataset -- or the state of the system at time t_i. For example, sample i from a movement is represented by the vector $x_i = (\xi_{i,1}, \xi_{i,2}, \dots, \xi_{i,p})$ where p represents the dimensionality of the input -- or the number of biomechanical variables. Each node in the output layer has an associated weight vector. For example, node j is represented by $y_j = (\eta_{j,1}, \eta_{j,2}, \dots, \eta_{j,p})$, notice that the dimensionality of the weight vectors and the input vectors must be equal. The nodes in the input layer are connected to all nodes in the output layer and nodes in the output layer are connected to adjacent nodes by a neighborhood relation. The space spanned by the weights is a Euclidean space, thus the distance calculated between a weight vector and an input vector is a Euclidean distance.
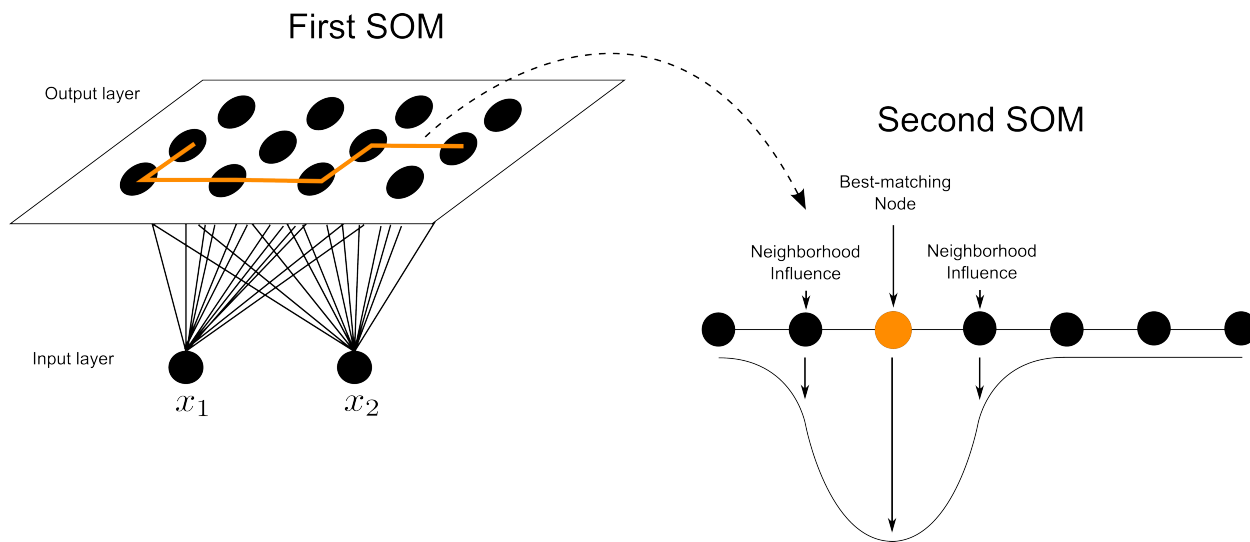

Figure 2. Connections between the nodes of the input and output layers are shown on the left. A sequence of inputs can be represented by a trajectory (orange line) connecting the consecutive best matching output nodes, which is a low-dimensional mapping of the high-dimensional input data. The coordinates of the trajectories are used as input to a second SOM, which is used to construct an attractor visualization. Stretching a theoretical horizontal line downwards according to node hit frequency and proximity of neighboring nodes creates basins of attraction, and illustrates a tendency towards the recruitment of similarly patterned movements.

SOM algorithm. The steps for training a SOM are as follows:

Initialization. Map dimensions, training parameters and initial values for weight vectors are chosen. The initial values and parameters are commonly based on PCA of the dataset, and are thus data driven (see Vesanto et al., 2000).

Find best matching node. Each input node will be *best represented* by a single node in the output whose weight vector has the shortest Euclidean distance to the given input vector. This output node is deemed the *best matching node*.

Update weights. SOMs use a competitive learning strategy in which the best matching node's weights are adjusted to become more similar to the respective input vector (see Vesanto et al., 2000 for batch training algorithm for weight updates). The weights of the neighboring nodes are also updated based on the neighborhood function which has a decreasing influence as proximity to the best matching node decreases.

Iteration. The previous two steps are repeated until the end of the user defined training period.

Map quality can be checked based on two quality measures: quantization error and topographical error. Quantization error represents the average Euclidean distance between all input vectors and their respective best matching nodes, which is a type of goodness of fit measure (Vesanto et al., 2000). Topographical error provides an indication of the tendency for the second-best matching node to be a neighbor of the best matching node (Kiviluoto, 1996). Training parameters should be set to minimize these two quality measures.

Visualization of the output. The nodes in the output layer can be ordered and arranged on a grid for visualization (e.g., Bauer & Schöllhorn, 1997); with this grid space visualization the axes are indices to nodes. One major shortcoming of the grid space visualization is that the Euclidean distance between the weight vectors of neighboring nodes appears to be equally distributed throughout the output layer. Since this is not the case, the U-matrix is commonly used, which is a hybrid grid space/weight space visualization which orders the nodes on a grid and also uses colored *distance* cells to represent the Euclidean distance between neighboring nodes (Vesanto & Alhoniemi, 2000). We have extended the U-matrix slightly by plotting a three-dimensional surface instead of a two-dimensional grid and coloring the surface by interpolating the colors of the distance cells. The z-axis also represents Euclidean distance between neighboring nodes and serves to enhance the visualization. Valleys on the U-matrix therefore are colored blue and represent nodes with similar weight vectors as their neighbors. Peaks, or ridges, are brightly colored (red or orange) and represent relatively large Euclidean distances between neighboring nodes.

Since the input data consists of several walking and running strides, the time-series change in coordination states can be simulated by superimposing a trajectory on the U-matrix connecting consecutive best matching nodes. The U-matrix and trajectory simulation can therefore visualize the changing coordination of a single movement and we can compare that trajectory to other movements. This approach differs from a conventional cluster analysis in that the phases of the movement, or the time-series change in coordination, which contribute to the clustering can easily be visualized.

Second SOM Analysis

As a second stage in the analysis each entire stride is classified with respect to the other strides in the dataset. In order to classify each stride we feed the output of the original trained SOM to a second SOM (often referred to as a second layer). Instead of using the weight vectors of the output nodes for training data (which are high-dimensional), we project the best matching nodes into weight space using Sammon's mapping technique (Sammon, 1969) and the two-dimensional coordinates in weight space of the best matching nodes for each stride are fed into a second SOM. Whereas Diedrich and Warren (1995) proposed a hypothetical potential landscape on which a function representing a system's attractor layout, with relative phase used as a collective variable and speed as a control variable could be plotted, we use the second SOM to empirically plot an attractor landscape using speed as the control parameter and the original SOM trajectory as a collective variable.

The topology of the output layer of the second SOM is a one-dimensional string of nodes and is visualized as an attractor diagram or landscape. Each node in the output can represent any number of strides in the original input data. When an output node is activated by best representing a given stride a theoretical line is stretched below horizontal by one (arbitrary) unit. Neighborhood nodes also stretch the line down according to their Euclidean distance from the best matching node. The visualization therefore represents the potential for similarly patterned movements to be recruited. The depth of the basin is determined by the frequency of node hits and also the similarity of neighboring nodes and their hit frequencies for a given speed (Figure 2). The nodes on opposite ends of the attractor diagrams represent the greatest dissimilarity between coordination patterns: we expected these to be associated with the fastest and slowest treadmill speeds. Kelso and colleagues (see Kelso, 1995) originally proposed the relative phase as a collective variable for bimanual coordination and others have used variants of relative phase for studying coordination in gait (e.g., Diedrich & Warren, 1995; Kao et al., 2003), we propose that the coordination involved with gait is far more complex than bi-manual coordination and requires collective variables which capture the dimensionality of coordination.

Coordination Variability

Each trajectory on the U-matrix consists of a sequence of best matching nodes of length n, which is equal to the number of time samples per set of gait strides, or gait cycles. The dimensionality, p, of the weight vectors associated with each best matching node is equal to the number of variables, or dimensions, of the input. The variability between trajectories on the U-matrix for the gait cycles at a given speed was calculated in three steps. First, the Euclidean distance between all strides being compared at each best

matching node, i, was calculated. Secondly, the average Euclidean distance was calculated for each row in the resulting distance matrix. Finally, total trajectory variability was calculated as the sum of the n time samples from the previous step (for more details see Lamb, Bartlett, Lindinger, & Kennedy, *2014*).

<div align="center">

Results

</div>

U-Matrices

Separate U-matrices were created for the three procedures (Figures 3 and 4 for the steady state and transient part of the mixed procedure, respectively). In all U-matrices there are two low, blue areas, or valleys, representing nodes with short Euclidean distances to their neighbors. These valleys are separated by brightly colored ridges, which correspond to high weight space differences between neighboring nodes. The valleys represent the walking and running patterns. Figure 3 shows the U-matrix for the participant's preferred walking (5.1 km/h; orange trajectory) and running (12.6 km/h; yellow trajectory) speeds in the steady state procedure. At no speeds did the trajectories cross the ridges in the steady state procedure. The same was true for increasing speed in the transient procedure. For the steady state part of the mixed procedure, U-matrix trajectories were very similar to those for the steady state procedure; the increasing speed transient U-matrices were also very similar to those for the transient procedure. However, for decreasing belt speeds in both, the transient procedure and transient part of the mixed procedure, the U-matrices showed trajectories both sides of, and some crossing, the ridges of high weight space difference. For example, for the transient decreasing speeds in the mixed procedure, crossings of the ridges of high weight space occurred for all speeds between 8.1 km/h (Figure 4A) and 7.7 km/h (Figure 4B) and also at 8.3 km/h and 8.4 km/h but not at 8.2 km/h at which a running pattern was evident (Figure 4C).
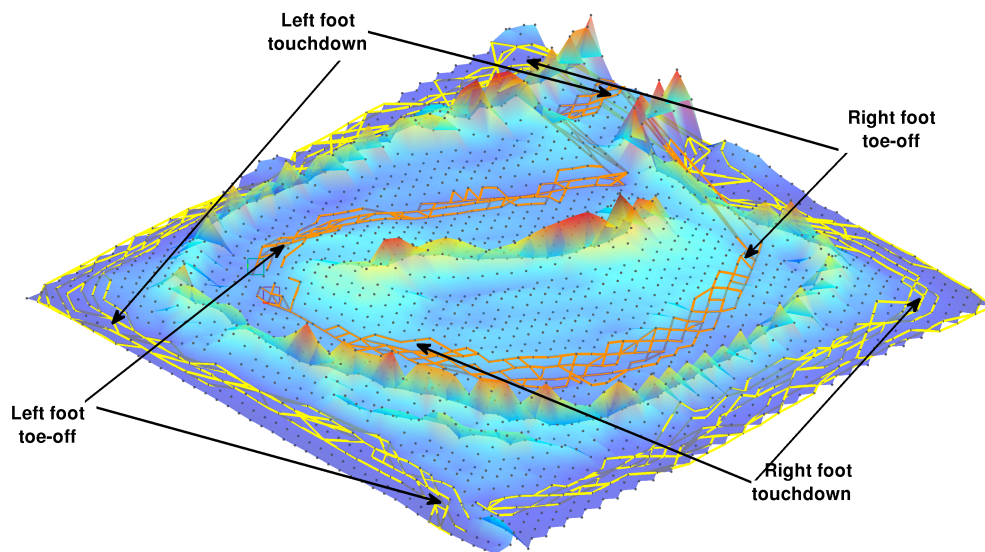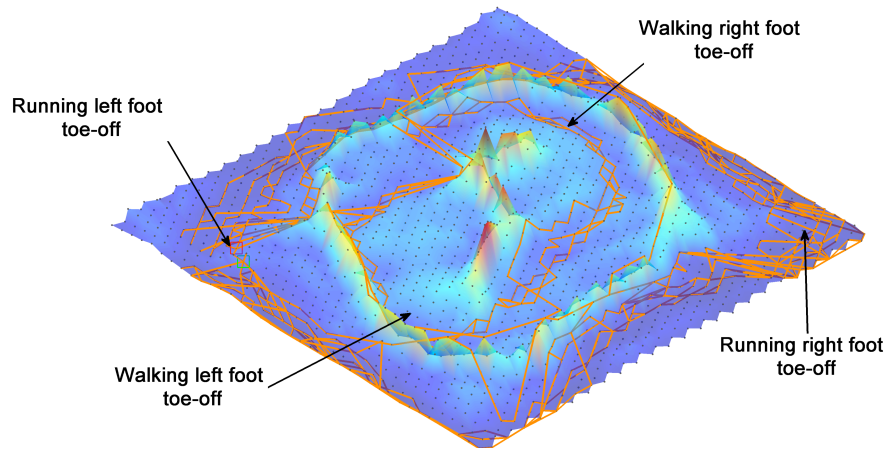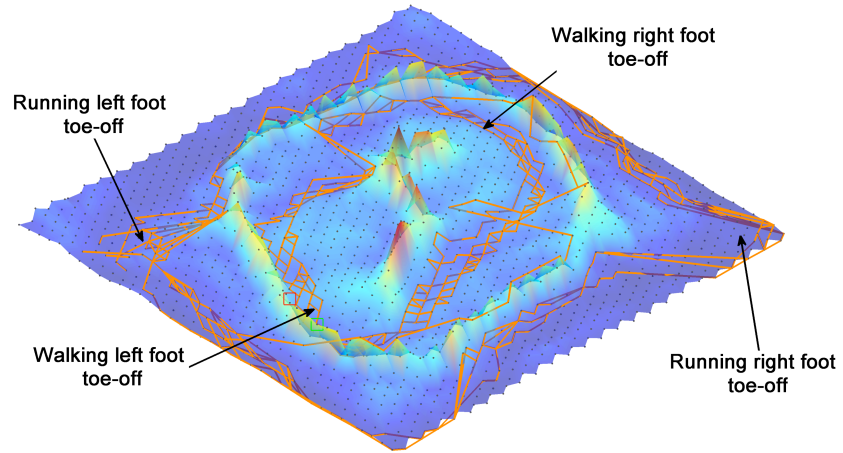

Figure 3. U-matrix for steady state procedure, the preferred walking speed of 5.1 km/h shown with the orange trajectory, and the preferred running speed of 12.6 km/h with the yellow trajectory. Events of the movement are also shown.
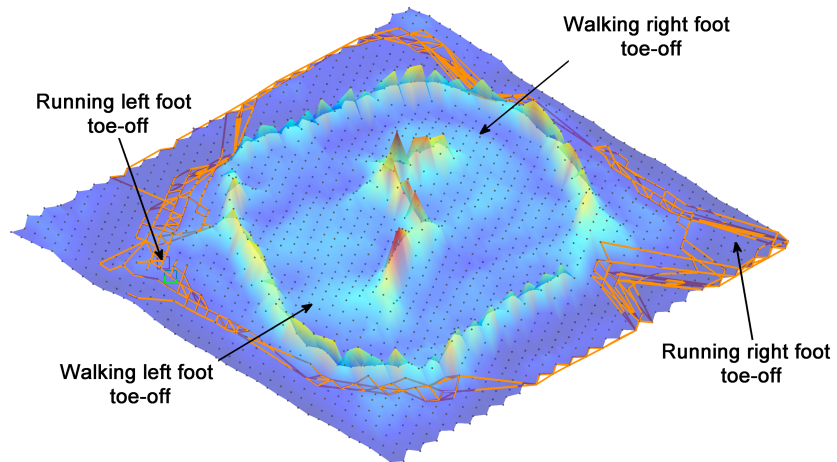
A

B

C

Figure 4. U-matrix for decreasing belt speed at: A: 8.1 km/h (top left); B: 7.7 km/h (top right); C: 8.2 km/h in the transient part of the mixed procedure.

Attractor Diagrams

The participant walked fluently at speeds up to and including 7.5 km/h and ran fluently at all speeds at and above 8.0 km/h in the steady state procedure. The attractor diagrams at each speed all showed a single basin of attraction, those for walking and running occupied different regions of the SOM output, one being a mirror image about the vertical axis of the other (Figure 5).
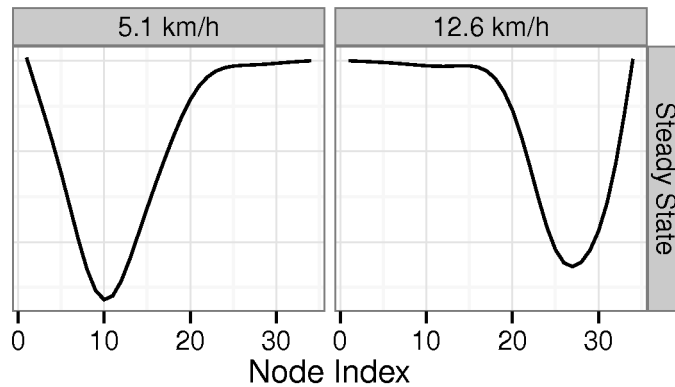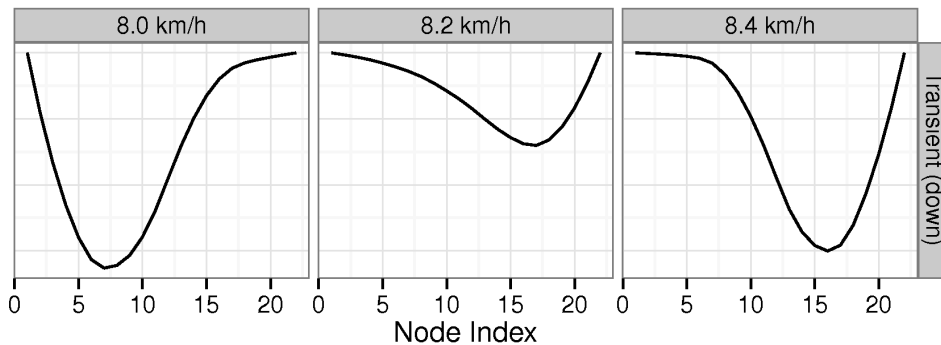

Figure 5. Basins of attraction for: preferred walking speed of 5.1 km/h (left); preferred running speed of 12.6 km/h (right) in the steady state procedure. The horizontal axis is the node index and the vertical axis is the relative frequency (arbitrary units) of activated nodes on the second SOM.
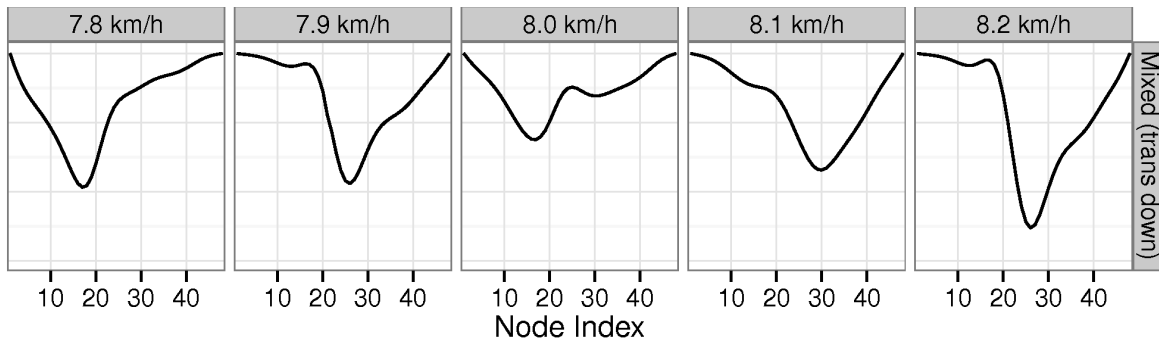
A

B

Figure 6. Basins of attraction for decreasing belt speed at: A: 8.0 km/h, 8.2 km/h and 8.4 km/h in the transient procedure; and B: 7.8 km/h, 7.9 km/h, 8.0 km/h, 8.1 km/h and 8.2 km/h in the transient part of the mixed procedure.

In the transient procedure, a similar result was found for increasing speed; however, for decreasing speed at 8.2 km/h, instability was evident in the form of a much shallower basin of attraction than at the previous speed, 8.4 km/h (Figure 6A). At the next speed down, 8.0 km/h, a walking attractor appeared.

In the deceasing speed transient part of the mixed procedure, there was much more variability through the transition zone (Figure 6B). At 8.0 km/h two basins of attraction were evident. When we plotted attractor landscapes (three-dimensional attractor diagrams with speed as the third axis) for this part of the mixed procedure, all speeds can be seen and an unstable region was evident around 8.0 km/h. In this region weak attractors appeared at one speed then disappeared and reappeared as the speed changed (Figure 7). Such a phenomenon was not seen in either of the other procedures or for increasing speed in the mixed procedure.

Coordination Variability

For the steady state procedure (Figure 8; note that the variability scale was chosen to facilitate comparison of Figures 10 and 11), multi-dimensional coordination variability between strides (the total trajectory variability – expressed as weight differences in the SOM trajectories) - was slightly higher at slow walking speeds, decreased at faster walking speeds, increased slightly towards and through the transition from walking to running and decreased again as the running speed increased. For the steady state condition in the third, mixed, procedure, the trend was somewhat similar (Figure 9). For increasing speeds, however, there was far less of an increase in variability across the whole region for which the U-matrix for the transient condition suggested some instability. For decreasing speeds, the variability rose from the fastest speeds to 9 and 8.6 km/h, dropped slightly then rose again at some, but not all, of the speeds in the transition region, then dropped again for walking speeds. In none of the steady state conditions was there a clear increase towards and through the transition region and a decrease thereafter.
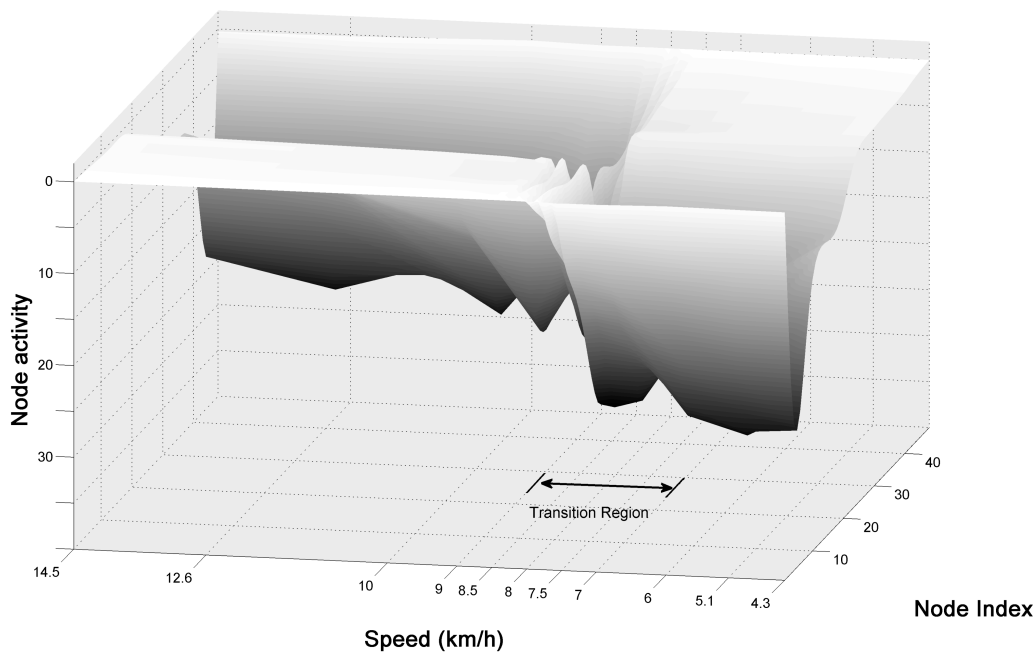

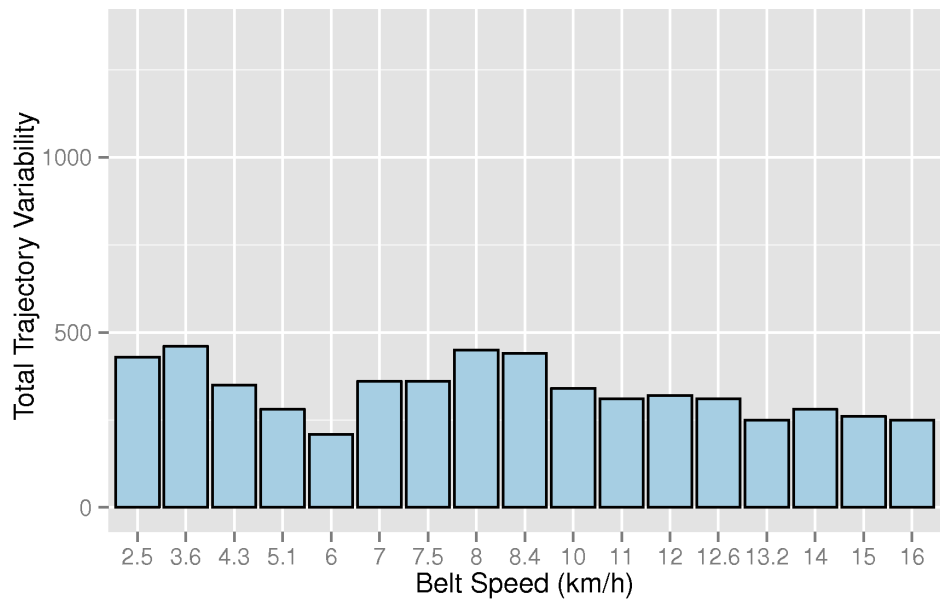*Figure 7.* Attractor landscape (or surface) for decreasing belt speed in the transient part of the mixed procedure.

Figure 8. Steady state multi-dimensional coordination variability (total trajectory variability) at various gait speeds.
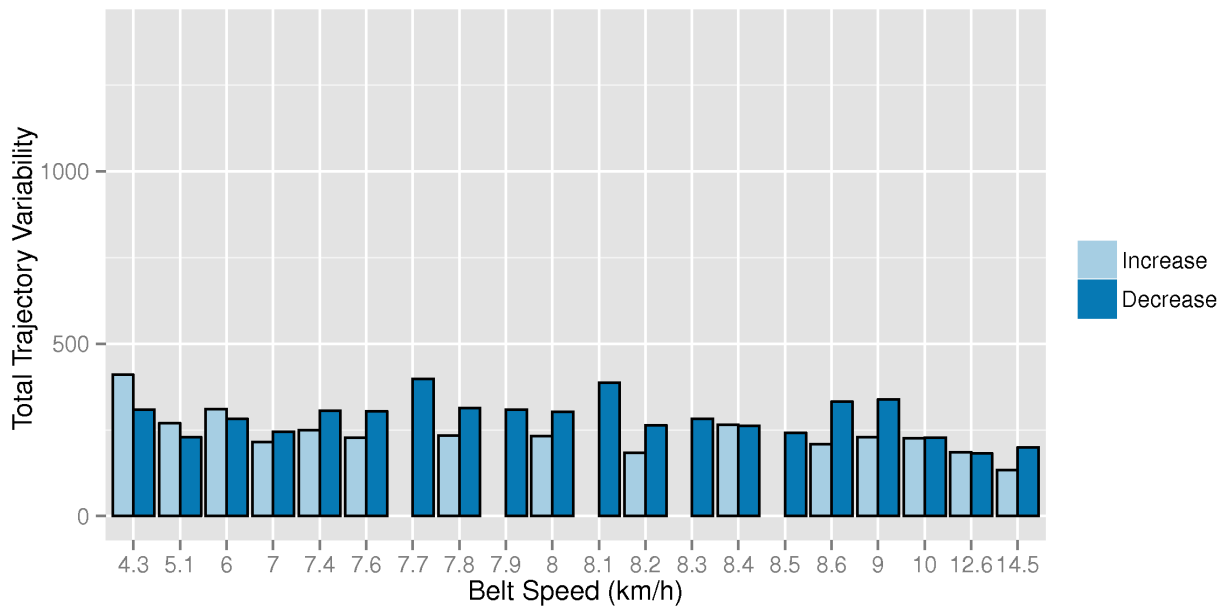

Figure 9. Steady state multi-dimensional coordination variability (total trajectory variability) at various gait speeds for the mixed procedure.
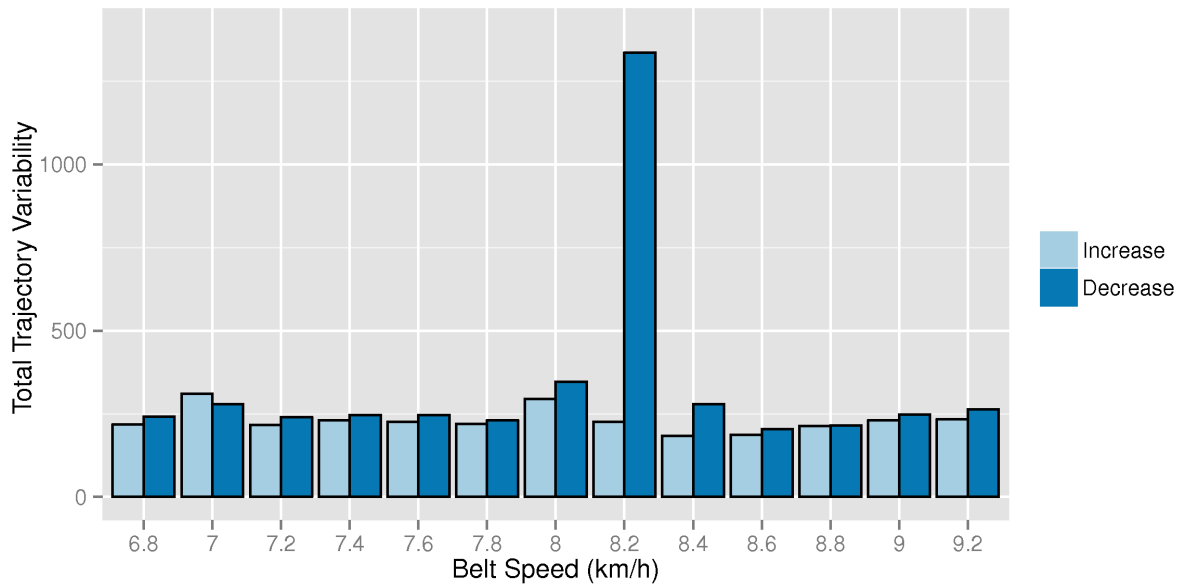
Figure 10. Transient multi-dimensional coordination variability (total trajectory variability) at various gait speeds for the transient procedure.

The transient conditions (the transient procedure and the transient part of the mixed procedure) showed rather different trends. In the transient procedure (Figure 10), the increasing speed condition showed little differences in magnitude or trends from the first, steady state, procedure. For decreasing speeds, however, a large peak variability – about four times greater than that at any other speed - was found for 8.2 km/h, in the transient region, with some evidence of a rise before that (see 8.4 km/h) and a tailing off thereafter (see 8 km/h).
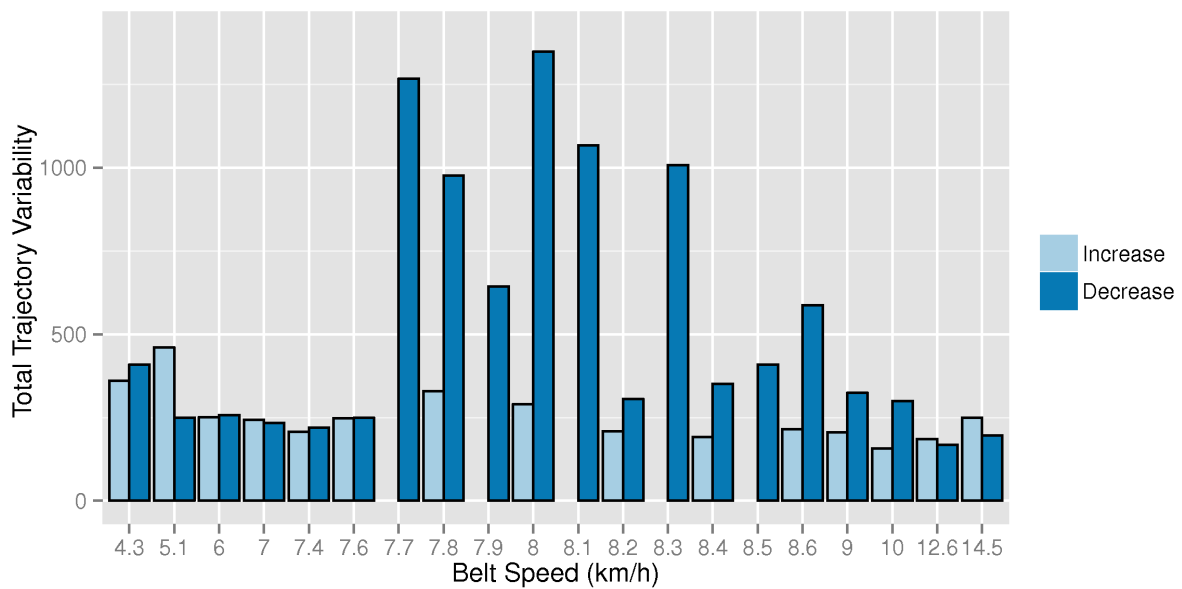

Figure 11. Transient multi-dimensional coordination variability (total trajectory variability) at various gait speeds for the mixed procedure.

In the transient part of the mixed procedure (Figure 11), the variability trend with increasing speed was similar to that for the steady state procedure (Figure 8) – a slight increase towards transition but with the largest values for slower walking. The decreasing speed procedure, however, showed large increases in variability during transition, these increases persisted, with some fluctuations, from 8.3 to 7.7 km/h; a rise towards transition from running was also apparent, although the large variability at 8.6 confounds that trend. There was a sharp decrease of variability as walking became established (from 7.6 km/h down).

Discussion

Coordination Stability and Instability

As is evident from the U-matrix figures and the attractor diagrams, the participant in this study was able to transition smoothly from a multi-dimensional walking coordination pattern to a running pattern with no instabilities evident in the steady state procedure and in the steady state condition in the mixed procedure. This was also true in the transient procedure and in the transient condition in the mixed procedure when the treadmill belt speed increased. However, there were instabilities at 8.2 and 8.0 km/h in her transition region when the belt speed decreased in the transient procedure – this was even more evident with smaller speed intervals in the mixed procedure. It appears the participant was uncertain whether to run or walk at those speeds. This instability was transient; when allowed time to adjust to new belt speeds in the mixed procedure, the participant walked or ran fluently at all belt speeds, as in the steady state procedure. This instability (or, some may prefer, multi-stability) was evident in two different ways, as follows.

Firstly, in the transient condition for the mixed procedure, two basins of attraction were clearly evident at 8.2 km/h. Two golfers in the study of Lamb et al. (2011) showed a similar complex transition between coordination patterns when chipping distance (the control parameter) increased as they changed from a short to a long chipping pattern, with one clearly showing multi-stability or instability; no instabilities were shown by the other two golfers. In light of those findings, we might expect that other runners would demonstrate different patterns of multi-dimensional stability – or instability - from those of the runner in this study.

Secondly, in the transient condition of the mixed procedure only, which was meant as a closer inspection of the peak in variability at 8.2 km/h in the transient procedure (decreasing belt speed), the participant had very 'short-lived' attractors clearly apparent at most 0.1 km/h increments in the transition region for decreasing speed (Figure 6B and 7). While the attractors on the left and right of the diagrams clearly represent walking and running, respectively, the middle of the diagrams represents a hybrid of the two gaits in which different phases of the gait cycle are in different modes of gait. Segers and colleagues (Segers et al., 2006; Segers, Lenoir, Aerts, & De Clercq, 2007) suggested an asymmetry during the transition in which, according to stride length and frequency, one leg was running and one was walking. Our results are similar in that the transition from running to walking involved coordination that was not walking or running, but had characteristics of both; this was shown by the U-matrix trajectories jumping across the ridge separating walking from running nodes (Figures 4A and 4B). At these transitions speeds, however, the phases of the gait cycle associated with a certain gait mode was variable from stride to stride; this was most clear from the variability in the attractor landscape during the transitions speeds (Figure 7). This type of instability might not have been evident in the transient procedure simply because the speed decrements were twice as large in the transition region in that procedure. Again, we would not expect this finding to apply to other runners, nor, necessarily, to the runner in our study on another occasion.

A further question arises; why could this runner transition smoothly from a stable walking attractor to a stable running attractor as the speed increased but not the other way round when the speed decreased? One explanation could be due to the participant being a competitive runner, for whom transient changes from walking to running are a part of every race, or training session, which is not so true for running to walking. It is noteworthy that the participant was not a recreation walker. For someone who walked competitively, or for long periods as a recreation, the findings might be different. An alternative explanation could be that the coordination involved with transitioning between gait modes is inherently different depending on whether speed is increasing or decreasing. We can only speculate that this might be the case; however, other researchers have suggested a 'functional hysteresis' (Segers et al., 2006; Segers et al., 2007) in that the speed at which the transition occurs did not depend on the direction of speed change but certain spatiotemporal and kinematic parameters changed in different ways with respect to the direction of speed change. Those authors showed that the transition from walking to running usually occurred during one step, while the transition from running to walking did not finish until two steps after the initiation of the transition.

Coordination Variability

The finding for steady state multi-dimensional coordination variability between strides was, basically, that it was somewhat higher at slow walking speeds, decreased somewhat at faster walking speeds, increased slightly towards and through the transition from walking to running or vice versa and decreased slightly again as the running speed increased or walking speed decreased. However, these changes were not consistent enough or large enough to follow the clear pattern reported by Kelso (1995) for bi-manual coordination, on which the functional role of variability in aiding coordination changes is, at least partly, based. The increase in coordination variability towards transition in the transient region for decreasing speeds, the fourfold increase in multi-dimensional variability in the transition region (for most speeds in the mixed procedure) and the decrease after transition were in agreement with previous research (e.g., Diedrich & Warren, 1995) that has reported an increase in two-joint coordination variability around the transition from running to walking. The results of this case study clearly disagree with the findings of Kao et al. (2003), even though their findings appear to be based on a transient procedure. It is worth noting that variability in continuous relative phase between pairs of joints was used by Kao et al. (2003): such "pairwise" variability and multi-dimensional variability may give contrary results. Furthermore, our case study design limits the extent to which our results can be compared to larger studies.

On Sagittal Plane Variables

We also found that the use of sagittal plane variables only was not able to demonstrate these results clearly and that cardan angles and angular velocities gave a much clearer picture. Therefore, reinterpretation of the results of studies of the walk-to-run transition that have used sagittal plane variables only (e.g., Kao et al., 2003, which used continuous relative phase based on sagittal plane hip, knee and ankle angles), or focused only on joint angles, as in Diedrich and Warren (1995), who used point-estimate relative phase which requires no angular velocity data, might be in order.

Conclusions

Studies which have looked at the transition between gait modes and have focused on low-dimensional coordination (and often sagittal plane variables) have reported conflicting results. From the perspective of pattern formation in self-organizing systems, increased variability was expected at transition speeds. We

found evidence for this as shown by U-matrix trajectory variability, but only for decreasing speeds in transient conditions. Further research concentrating on multi-dimensional coordination at small speed increments through the transition would be useful for helping substantiate our findings. Large studies with many participants would also help determine to what extent these characteristics of changes in coordination apply to other runners. SOMs have been shown to be a useful tool for exploring and visualizing human gait data and their continued use and development are likely to facilitate further understanding of coordination variability.

Acknowledgements

References

Bartlett, R. M., O'Donovan, D., Kennedy, G., & Saini, R. (2012). Are there coordination instabilities in the walk-to-run transition? A case study using self-organising maps. In E. Bradshaw, A. Burnett, & P. Hume (Eds.), *International Society of Biomechanics in Sports E-Proceedings, Volume 3: Oral Presentations*, pp. 329-332. Melbourne: Australian Catholic University. https://ojs.ub.uni-konstanz.de/cpa/article/view/5297

Barton, G., Lees, A., Lisboa, P., & Attfield, S. (2006). Visualisation of gait data with Kohonen self-organising neural maps. *Gait & Posture, 24*, 46-53. http://dx.doi.org/10.1016/j.gaitpost.2005.07.005

Bauer, H. U., & Schöllhorn, W. I. (1997). Self-organizing maps for the analysis of complex movement patterns. *Neural Processing Letters, 5*, 193–197. http://dx.doi.org/10.1023/A%3A1009646811510

Begon, M., Monnet, T., & Lacouture, P. (2007). Effects of movement for estimating the hip joint center. *Gait & Posture, 25*, 353-359. http://dx.doi.org/10.1016/j.gaitpost.2006.04.010

Diedrich, F. J., & Warren, W. H. (1995). Why change gaits? The dynamics of the walk-to-run transition. *Journal of Experimental Psychology: Human Perception and Performance*, *21*, 182-202. http://citeseerx.ist.psu.edu/viewdoc/download?doi=10.1.1.212.188&rep=rep1&type=pdf

Diedrich, F. J., & Warren, W. H. (1998). The dynamics of gait transitions: Effects of grade and load. *Journal of Motor Behavior, 30*, 60-78. http://dx.doi.org/10.1080/00222899809601323

Haddad, J. M., van Emmerik, R. E. A., Whittlesey, S. N., & Hamill, J. (2006). Adaptations in interlimb and intralimb coordination to asymmetrical load in human walking, *Gait & Posture, 23*, 429-434. http://dx.doi.org/10.1016/j.gaitpost.2005.05.006

Haken, H., Kelso, J. A. S., & Bunz, H. (1985). A theoretical model of phase transitions in human hand movements. *Biological Cybernetics*, *51*, 347-356. http://www.ncbi.nlm.nih.gov/pubmed/3978150

Hamill, J., Haddad, J. M., & McDermott, W. J. (2000). Issues in quantifying variability from a dynamical systems perspective, *Journal of Applied Biomechanics, 16*, 407-418.

Kao, J. C., Ringenbach, S. D., & Martin, P. E. (2003). Gait transitions are not dependent on changes in intralimb coordination variability, *Journal of Motor Behavior, 5*, 211-214. http://www.ncbi.nlm.nih.gov/pubmed/12873836

Kelso, J. A. S. (1995). *Dynamic patterns: The self-organization of brain and behavior*. Cambridge, MA: MIT Press.

Kiviluoto, K. (1996). Topology preservation in self-organising maps. *IEEE International Conference on Neural Networks, 1*, 294–299. http://dx.doi.org/http://dx.doi.org/10.1109/ICNN.1996.548907

Kohonen, T. (2001). *Self-organizing maps* (3rd ed.). Berlin, Germany: Springer.

Kohonen, T. (1982). Self-organized formation of topologically correct feature maps, *Biological Cybernetics, 43*, 59-69. http://dx.doi.org/10.1007/BF00337288

Lamb, P. F., Bartlett, R. M., Lindinger, S., & Kennedy, G. (2014). Multi-dimensional coordination in cross-country skiing analyzed using self-organizing maps. *Human Movement Science, 33,* 54-69. http://dx.doi.org/10.1016/j.humov.2013.08.005

Lamb, P. F., Bartlett, R. M., & Robins, A. (2011). Artificial neural networks for analyzing inter-limb coordination: The golf chip shot. *Human Movement Science*, *30*, 1129-1143. http://dx.doi.org/10.1016/j.humov.2010.12.006

Lamb, P. F., Bartlett, R. M., & Robins, A. (2010). Self-organizing maps: An objective method for clustering complex human movement. *International Journal of Computer Science in Sport, 9,* 20-29.

Lamoth, C. J. C., Daffertshofer, A., Huys, R., & Beek, P. J. (2009). Steady and transient coordination structures of walking and running. *Human Movement Science*, *28*, 371-386. http://dx.doi.org/10.1016/j.humov.2008.10.001

Li, L., van den Bogert, E. C. H, Caldwell, G. E., van Emmerik, R. E. A, & Hamill, J. (1999). Coordination patterns of walking and running at similar speed and stride frequency. *Human Movement Science*, *18*, 67-85. http://dx.doi.org/10.1016/S0167-9457(98)00034-7

Sammon, J. W. (1969). A nonlinear mapping for data structure analysis. *IEEE Transactions on Computers, C-18,*, 401–409. http://dx.doi.org/10.1109/T-C.1969.222678

Seay, J. F., Haddad, J. M., van Emmerik, R. E., & Hamill, J. (2006). Coordination variability around the walk to run transition during human locomotion. *Motor Control*, *10*, 178-196. http://www.ncbi.nlm.nih.gov/pubmed/16871012

Segers, V., Aerts, P., Lenoir, M., & De Clercq, D. (2006). Spatiotemporal characteristics of the walk-to-run and run-to-walk transition when gradually changing speed. *Gait & Posture*, *24,* 247–254. http://dx.doi.org/10.1016/j.gaitpost.2005.09.006

Segers, V., Lenoir, M., Aerts, P., & De Clercq, D. (2007). Kinematics of the transition between walking and running when gradually changing speed. *Gait & Posture*, *26*, 349–361. http://dx.doi.org/10.1016/j.gaitpost.2006.10.013

Schwartz, M. H., & Rozumalski, A. (2005). A new method for estimating joint parameters from motion data. *Journal of Biomechanics*, *38*, 107-116. http://dx.doi.org/10.1016/j.jbiomech.2004.03.009

Vesanto, J., & Alhoniemi, E. (2000). Clustering of the self-organizing map. *IEEE Transaction on Neural Networks, 2*, 586-600. http://lib.tkk.fi/Diss/2002/isbn951226093X/article4.pdf

Vesanto, J., Himberg, J., Alhoniemi, E., & Parkankangas, J. (2000). SOM Toolbox for MATLAB 5. Technical Report. Helsinki University of Technology, Helsinki. http://www.cis.hut.fi/somtoolbox/